

Measures of neural similarity

Bobadilla-Suarez, S. ^{a,d,*}, Ahlheim, C. ^{a,d}, Mehrotra, A. ^{b,d}, Panos, A. ^{c,d},
Love, B. C. ^{a,d}

^a*Department of Experimental Psychology, University College London, 26 Bedford Way, London, UK, WC1H 0AP*

^b*Department of Geography, University College London, Gower Street, London, WC1E 6BT*

^c*Department of Statistical Science, University College London, Gower Street, London, WC1E 6BT*

^d*The Alan Turing Institute, 96 Euston Road, London, UK, NW1 2DB*

Abstract

One fundamental question is what makes two brain states similar. For example, what makes the activity in visual cortex elicited from viewing a robin similar to a sparrow? One common assumption in fMRI analysis is that neural similarity is described by Pearson correlation. However, there are a host of other possibilities, including Minkowski and Mahalanobis measures, with each differing in its mathematical, theoretical, neural computational assumptions. Moreover, the operable measures may vary across brain regions and tasks. Here, we evaluated which of several competing similarity measures best captured neural similarity. Our technique uses a decoding approach to assess the information present in a brain region and the similarity measures that best correspond to the classifier's confusion matrix are preferred. Across two published fMRI datasets, we found the preferred neural similarity measures were common across brain regions, but differed across tasks. Moreover, Pearson correlation was consistently surpassed by alternatives.

Keywords: neural similarity, neural coding, machine learning, fMRI

^{*}Corresponding author

Email address: sebastian.suarez.12@ucl.ac.uk (Bobadilla-Suarez, S.)

1. Introduction

2 Detecting similarities is critical to a range of cognitive processes and tasks,
3 such as memory retrieval, analogy, decision making, categorization, object
4 recognition, and reasoning [1, 2, 3, 4, 5, 6]. Key questions for neuroscience
5 include which measures of similarity does the brain use, and do similarity
6 computations differ across brain regions and tasks. Whereas psychology has
7 considered a dizzying array of competing accounts of similarity [7, 8, 9, 10,
8 11, 12, 13], research in neuroscience usually assumes that Pearson correlation
9 captures the similarity between different brain states [14, 15, 16, 17, 18, 19,
10 20, 21]), though see [22, 23, 24, 16].

11 On the face of it, it seems unlikely that the brain would use a single mea-
12 sure of similarity across regions and tasks. First, across regions, the signal
13 and type of information represented can differ [6, 25, 26], which might lead
14 the accompanying similarity operations to also differ. Second, task differ-
15 ences, such as those that shift attention [27, 28, 29], lead to changes in the
16 brain’s similarity space which may reflect basic changes in the underlying
17 similarity computation. Outside neuroscience it is common to use different
18 similarity measures on different representations. For example, in machine
19 learning, Euclidean measures are often used to determine neighbors in im-
20 age embeddings whereas cosine similarity is more commonly used in natural
21 language processing [30].

22 In this contribution, we developed a technique to address two specific
23 goals. The first goal was to ascertain whether the similarity measures used by
24 the brain differ across regions. The second goal was to investigate whether the
25 preferred measures differ across tasks and stimulus conditions. Our broader
26 aim was to elucidate the nature of neural similarity.

27 Previous studies have adopted different similarity measures to relate pairs
28 of brain states such as Pearson correlation or the Mahalanobis measure [31,
29 32, 33, 14]. However, the basis for choosing one measure over another is not
30 always clear. The choice of measure induces a host of assumptions, including
31 assumptions about how the brain codes and processes information. While
32 all the measures considered operate on two vectors associated with two brain
33 states (e.g., the BOLD response elicited across voxels when a subject views
34 a truck vs. a moped), the operations performed when comparing these two
35 vectors differ for each similarity measure.

1 *1.1. Families of similarity measures*

2 To better understand these assumptions and their importance, we or-
3 ganise common measures of similarity, many of which are used in the neu-
4 roscience literature, into three families (see Figure 1, left side). The most
5 basic split is between similarity measures that focus on the angle between
6 vectors (e.g., Pearson correlation or cosine distance) and measures that focus
7 on differences in vector magnitudes. The latter branch subdivides between
8 distributional measures that are sensitive to covariance across vector dimen-
9 sions (e.g., Mahalanobis) and those that are not (e.g., Euclidean). Of course
10 there are uncountably infinite similarity measures one could choose to assess;
11 the goal here is to compare common measures that can discriminate between
12 different computations of interest as organized by these families of measures
13 with focus on angle, magnitude, and distributional properties.

14 The choice of similarity measure can shape how neural data are inter-
15 preted. Consider the right panel in Figure 1. In this example, the neural
16 representation of object **a** is more similar to that of **b** than **c** when an angle
17 measure is used, but this pattern reverses when a magnitude measure is used.

18 Unlike the other measures, distributional measures are anisotropic, mean-
19 ing the direction of measurement is consequential.¹ Examples of such mea-
20 sures are variation of information, Mahalanobis, and Bhattacharyya mea-
21 sures. These measures consider the covariance between stimuli dimensions,
22 which implies that the direction (in feature or voxel space) along which the
23 measurement is made will impact the measurement itself.

24 The choice of similarity measure reflects basic assumptions about the na-
25 ture of the underlying neural computation. For example, Pearson correlation
26 (a common measure for neural similarity in fMRI, e.g., [14, 15, 16, 17, 18,
27 19, 20, 35]) assumes that overall levels of voxel activity are normalized and
28 that each voxel independently contributes to similarity, whereas Minkowski
29 measures assume similarity involves distances in a metrical space instead of
30 vector directions. Furthermore, the Mahalanobis measure expands on both
31 Minkowski and Pearson by assuming that the distributional pattern of voxel
32 activity is consequential.

33 Knowing which similarity measure best describes the brain’s operation
34 would not only improve data analyses, but could also illuminate the nature

¹Anisotropic measures should not be confused with asymmetric measures; the latter gives different values based on which stimulus is measured first [34, 7].

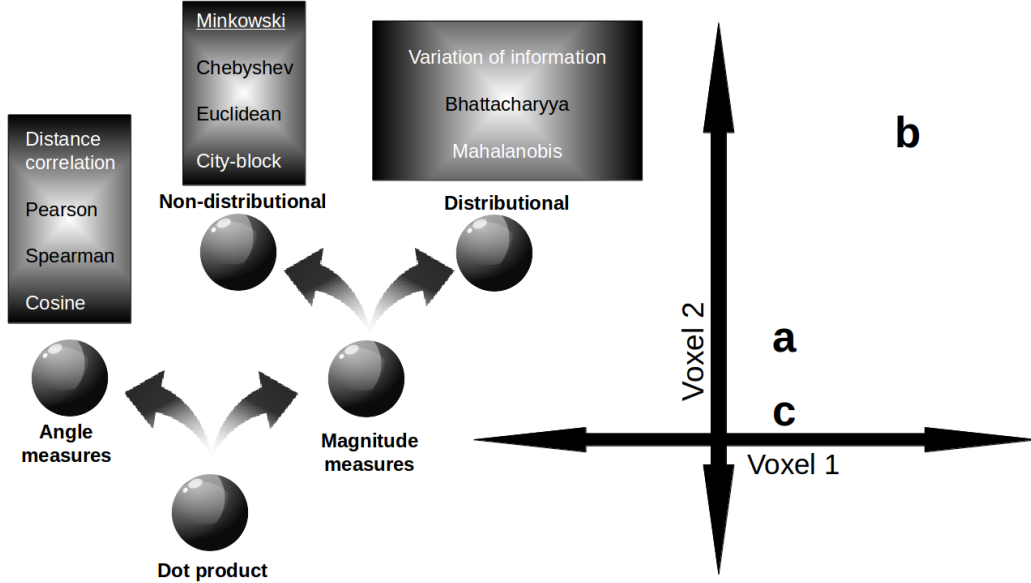


Figure 1: Families of similarity measures. (left panel) Similarity measures divide into those concerned with angle vs. magnitude differences between vectors. Pearson correlation and Euclidean distance are common angle and magnitude measures, respectively. The magnitude family further subdivides according to distributional assumptions. Measures like Mahalanobis are distributional in that they are sensitive to co-variance such that similarity falls more rapidly along low variance directions. (right panel) The choice of similarity measure can strongly affect inferences about neural representational spaces. In this example, stimuli **a**, **b**, and **c** elicit different patterns of activity across two voxels. When Pearson correlation is used, stimulus **a** is more similar to **b** than to **c**. However, when the Euclidean measure is used, the pattern reverses such that stimulus **a** is more similar to **c** than **b**.

1 of neural computation at multiple levels of analysis. For example, if a brain
 2 region normalized input patterns for key computations, then Pearson cor-
 3 relation might have superior descriptive power than the dot product. At a
 4 lower level, such a result would be consistent with mutually inhibiting single
 5 cells [36]. On the other hand, if the brain matches to a rigid template or filter
 6 (e.g., [37]), then the Euclidean measure should provide a better explanation
 7 for neural data.

8 To identify which similarity measures are used by the brain requires ad-
 9 dressing a number of challenges. One challenge is to specify a standard by
 10 which to evaluate competing similarity measures. Related work in Psychol-
 11 ogy and Neuroscience has relied on evaluating against verbal report. How-

1 ever, such an approach is not suited to our aims because we are interested
2 in neural computations that may differ across brain regions and which may
3 not be accessible by verbal report or introspection.

4 Instead, we rely on a decoding approach to assess the information latent
5 in a brain region. The intuition is that brain states that are similar should be
6 confusable in decoding. For example, a machine classifier may be more likely
7 to confuse the brain activity elicited by a bicycle with that by a motorcycle
8 than a car. In this fashion, we can evaluate competing similarity measures
9 on a per region basis in a manner that is not constrained by verbal report.
10 The insight that similarity is intimately related to confusability has a long
11 and rich intellectual history [38, 39, 40] though has not yet been considered
12 to evaluate what makes two brain states similar.

13 *1.2. Discrimination of similarity measures*

14 Our method for distinguishing the similarity measure used by the brain
15 involves two basic steps:

- 16 1. For each ROI, compute a pairwise confusion matrix using a classifier.
17 For each ROI, also compute a similarity matrix for each candidate
18 similarity measure.
- 19 2. For each similarity measure, correlate its similarity matrix with the
20 confusion matrix using Spearman correlation to avoid scaling issues.

21 The better a similarity measures characterizes what makes two brain
22 states similar, the higher its Spearman correlation with the confusion matrix
23 should be. This analysis uses the confusion matrix as an approximation of
24 what information is present in a brain region (more on this below).

25 The matrices for each similarity measure were optimized to maximize
26 the Spearman correlation with the confusion matrix by performing feature
27 selection on voxels (see Figure 2). See the SI (Supplemental Information)
28 for details on the similarity measures. Importantly, to understand the re-
29 sults, some similarity measures that estimate covariance matrices are tagged
30 according to the type of regularization used; with (d) for keeping only the
31 diagonal entries and (r) for Ledoit-Wolf shrinkage.

32 We considered all 110 regions of interest (see SI for a list of the 110
33 regions) from the Oxford-Harvard Brain Atlas (provided with FSL, [41]) for
34 two previously published datasets. One dataset was from a study in which
35 participants viewed geometric shapes (GS) [28] and the other dataset was

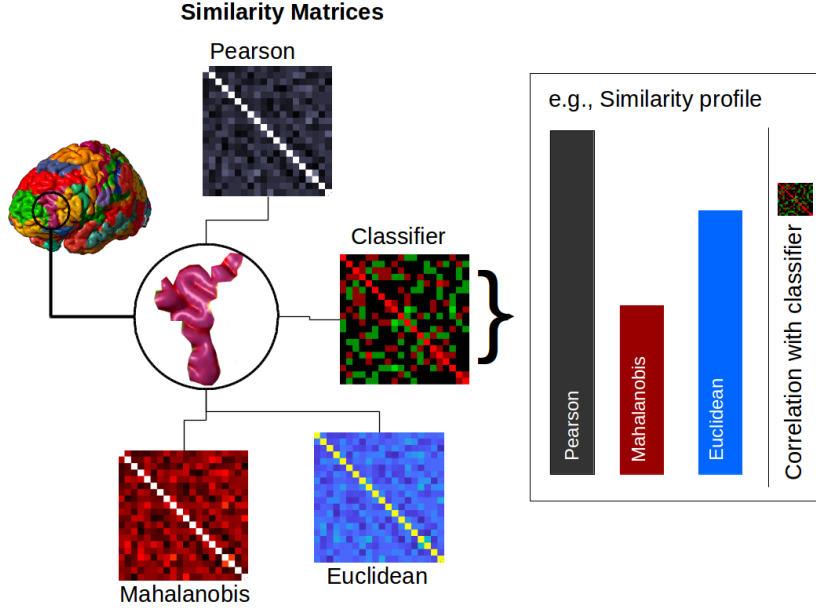


Figure 2: Evaluating the similarity profile for a ROI. The confusion matrix from a classifier is used to approximate the information present in the ROI. The similarity matrix from each similarity measure is correlated with this confusion matrix (i.e., the classifier matrix in the figure). The pattern of these correlations (i.e., the performance of the various similarity measures) is the similarity profile for that ROI. Similarity profiles can be compared between ROIs, both within and between datasets (see Materials and Methods section for more details).

1 from a study in which participants viewed natural images (NI) [6]. For
2 each dataset, we determined the top 10 ROIs for decoding accuracy (cf.
3 Bhandari et al. [42]). The union of these top ROIs provided 12 ROIs that
4 were considered in subsequent analyses (see SI).

5 *1.3. Lower confusability as information gain*

6 As mentioned above, our proposed method involves approximating brain
7 state information with a classifier. Subsequently, we use this approxima-
8 tion to assess an array of similarity measures. The motivation for using a
9 classifier to approximate information in a brain state arises from an infor-
10 mation theoretic perspective. For example, suppose one's prior assumption
11 is that two stimuli are equally likely, which corresponds to random guess-
12 ing or maximal entropy (1 bit). If a probabilistic classifier with the same
13 prior is applied to the stimulus and approaches 100% accuracy, then the

1 information gain approaches 1 bit. Formally, one can measure the Kullback-
2 Leibler (KL) divergence (a continuous, non-saturating measure) between a
3 prior distribution p (centered at 0.5) and an updated distribution q defined
4 by the classifier’s output. With a suitable prior distribution for the classi-
5 fier, the KL-divergence is always defined and enables a computable measure
6 of brain state information. Thus, KL-divergence, or information gain, will
7 be inversely proportional to confusability as measured by the classifier. Of
8 course, in practice, machine classifiers do not reach close to 100% accuracy
9 with fMRI data for the types of discriminations that we consider. The point
10 is that decoding and measuring available information in a brain state are
11 intimately linked.

12 *1.4. Classification is not similarity*

13 Although it should be clear cognitive scientists of all varieties that simi-
14 larity and classification are conceptually distinct (see [2]), it may not be as
15 apparent to some neuroscientists whose focus is elsewhere. To view simi-
16 larity and classification as one in the same, would be akin to viewing any
17 operation in which similarity could be relevant, such as memory retrieval, as
18 synonymous with similarity [1].

19 Mathematically, the domain and range of similarity and classification
20 functions are distinct. Similarity takes as its domain (i.e., input) two states
21 and its range (i.e., output) is a scalar value (i.e., the similarity). Notice that
22 similarity can apply to any two states, irrespective of class membership. A
23 similarity function does not need to be “trained” and “tested” on a particular
24 discrimination, but instead can apply broadly. In contrast, a classification
25 function takes as its domain (i.e., input) items drawn from a predetermined
26 set of classes and its range (i.e., output) is a nominal value indicating the class
27 membership of the item. A classifier is trained on items from the contrasting
28 classes and tested only on items drawn from these same distributions.

29 To showcase the distinction between similarly and classification opera-
30 tors, in addition to our main results, we also present a results for a non-
31 classification task that relies on neural similarity. In particular, we present
32 results for a triplet task in which we assess whether neural similarity between
33 a standard stimulus and two probe stimuli, one of which matches in shape.
34 The similarity measures that perform best in the triplet task are the ones that
35 perform best in our main decoding analyses. Critically, the stimulus classes
36 used in the triplet task were not included in the decoding analysis, which
37 highlights that similarity functions apply more broadly than classification

1 functions and that our method for selecting the brain's preferred similarity
2 functions generalizes to novel stimulus classes. Before visiting this result,
3 we present the main results that answer key questions, such as whether the
4 brain's preferred similarity measures are common across regions and tasks.

5 **2. Results**

6 *2.1. Neural similarity*

7 What makes two brain states similar and does it vary across brain re-
8 gions and tasks? The following analyses focus both on the performance of
9 individual similarity measures and on the pattern of performance across a
10 set of candidate measures, which we refer to as the *similarity profile* for an
11 ROI (see Figure 2).

12 As a precursor, we first tested whether similarity measures differed in their
13 performance (Figure 3a). Specifically, we evaluated whether certain measures
14 better describe what makes two brain states similar by nested comparison
15 using a mixed-effects model for each study (see Materials and Methods).
16 For both studies, similarity measures differed in their performance, $\chi^2(2) =$
17 1720.331, $p < 0.001$; $\chi^2(2) = 6770.249$, $p < 0.001$, for the GS and NI studies,
18 respectively.

19 We tested whether the similarity profile differed across brain regions
20 within each study. The similarity profiles (i.e., mean aggregate performance
21 across measures) were remarkably alike across ROIs (see Materials and Methods).
22 High (Pearson) correlations are presented within task for both the GS study
23 (Figure 3b) and the NI study (Figure 3c) between all pairs of ROIs; where
24 mean correlation of the upper triangle is 0.95 (s.d. = 0.034) in the former
25 and 0.96 (s.d. = 0.027) in the latter. Bartlett's test [43], which evaluates
26 whether the matrices are different from an identity matrix, was significant for
27 both the GS study, $\chi^2(66) = 432.847$, $p < 0.001$, and the NI study, $\chi^2(66)$
28 = 502.7494, $p < 0.001$. Permutation tests (with 10,000 iterations), where
29 the labels of the similarity measures were permuted, confirmed these results
30 ($p < 0.001$). These results are consistent with the same similarity measures
31 being used across brain regions within each study.

32 We tested whether similarity profiles differed between studies. The results
33 indicated that similarity profiles differed between studies, suggesting that
34 the operable neural similarity measures can change as a function of task or
35 stimuli (Figure 3d). In particular, similarity profiles between studies were
36 negatively correlated with a mean correlation of the upper triangle of -0.27

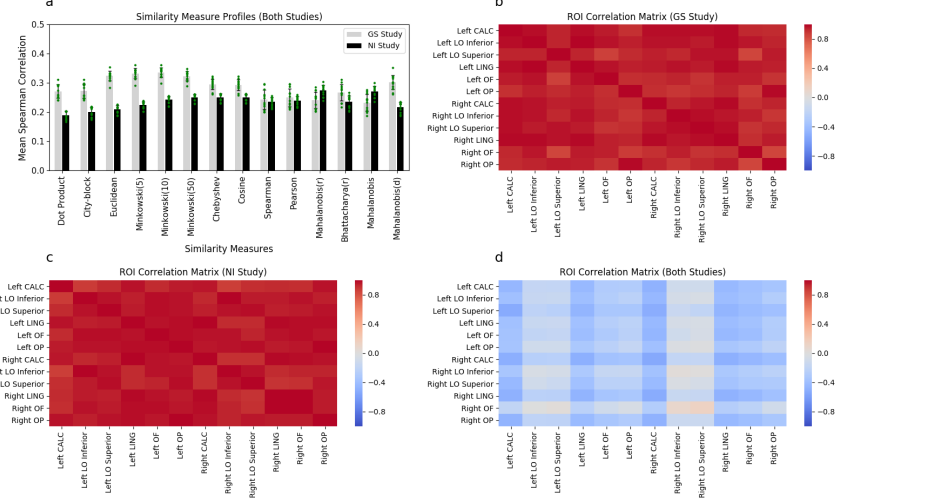


Figure 3: Similarity measure profiles and ROI correlation matrices. Mean Spearman correlations (a) for each similarity measure and the classifier confusion matrix in the GS study (grey bars) and the NI study (black bars) are displayed. To convey the variability, error bars are plotted as standard deviations and each ROI mean is plotted as a green point. ROI correlation matrices for the (b) GS and (c) NI studies, demonstrating that the similarity profiles were alike across brain regions (i.e., were positively Pearson correlated). ROI correlation matrix (d) demonstrating that the similarity profiles disagreed across studies (i.e., were negatively Pearson correlated). The 12 ROIs were left and right intracalcarine cortex (CALC), left and right lateral occipital cortex (LO) inferior and superior divisions, left and right lingual gyrus (LING), left and right occipital fusiform gyrus (OF), and left and right occipital pole (OP).

1 (s.d. = 0.148). Jennrich's test [44] showed that this matrix was different
2 than a matrix of zeros, $\chi^2(66) = 769.0349$, $p < 0.001$. Permutation tests
3 (10,000 iterations) with shuffling of similarity label measures also confirmed
4 these results ($p < 0.001$).

5 2.2. Searchlight analysis

6 In light of these results, *post hoc* pairwise tests of each similarity against
7 the Pearson similarity measure, which is the *de facto* default choice in the
8 literature, were conducted. The contrasts from the mixed effects models
9 (mentioned above, see Materials and Methods) presented in Table 1 pro-
10 vide evidence that some similarity measures are a superior description of the
11 brain's similarity measure. The performance of many measures differed from
12 Pearson, especially in the NI study. Notably, only two variants of the Ma-

GS Study		
Similarity measure	<i>z</i>	<i>p</i>
Minkowski(5)	12.562	< 0.001
Euclidean	12.145	< 0.001
Minkowski(10)	10.459	< 0.001
city-block	10.479	< 0.001
Mahalanobis(d)	8.825	< 0.001
Minkowski(50)	6.624	< 0.001
Chebyshev	6.353	< 0.001
cosine	4.532	< 0.001
dot product	4.053	< 0.001
Mahalanobis	(3.161)	0.02
NI study		
Similarity measure	<i>z</i>	<i>p</i>
Mahalanobis(r)	11.301	< 0.001
Mahalanobis	10.304	< 0.001
Minkowski(50)	4.920	< 0.001
Chebyshev	4.733	< 0.001
Minkowski(10)	4.005	< 0.001
Euclidean	(5.170)	< 0.001
Mahalanobis(d)	(7.593)	< 0.001
city-block	(10.411)	< 0.001
cosine	(22.803)	< 0.001
dot product	(29.547)	< 0.001

Table 1: Comparison of similarity measures to Pearson correlation. Top panel shows significant *z* statistics for measures worse than Pearson correlation (in brackets) and better than Pearson correlation for the GS study. Bottom panel shows the same for the NI study. *p*-values are Bonferroni corrected.

1 halanobis measure and three Minkowski measures outperformed Pearson. In
2 the GS study, we can observe that all the Minkowski distances performed
3 better than Pearson as well as cosine, Mahalanobis(d), and the dot product.
4 Once again, the contrasting pattern of results between the two studies is
5 striking.

6 Given the performance of the Euclidean and Mahalanobis(r) measures,
7 and that they have been used previously in analyzing neural data [16, 45, 46,
8 47], we selected these measures for inclusion in a searchlight analysis (Figure
9 4, see Materials and Methods for details). By comparing the Euclidean and
10 Mahalanobis(r) measures to Pearson correlation on a voxel-by-voxel basis
11 for the 12 ROIs, we aimed to provide a visualization of the performance
12 of similarity measures across regions and studies. Figure 4 illustrates the
13 regions where these two measures outperform Pearson correlation, displaying
14 the maximum t for voxels where both Euclidean and Mahalanobis overlap
15 (see SI for visualizations of the overlap).

16 In the NI study, the Mahalanobis(r) measure dominated (Figure 4b), con-
17 firming the results from the previous analyses. In contrast, in the GS study
18 (Figure 4a) Euclidean dominates in some regions whereas Mahalanobis(r)
19 dominates in others. Despite it being a *de facto* standard, Pearson similarity
20 was never the top measure. For this *post hoc* analysis, the measures were
21 compared using permuted paired sample t statistics for each voxel. Positive
22 t statistics that survived threshold-free cluster enhancement (TFCE) correc-
23 tion with $p < 0.001$ are presented in Figure 4 (see Materials and Methods
24 for the rationale behind this threshold).

25 2.3. Triplet task

26 As discussed in the Introduction, similarity and classification are distinct
27 concepts. To illustrate, we show how similarity measures can be used in
28 non-classification tasks involving stimuli from novel (untrained) classes. In
29 particular, we consider a triplet task involving data from the NI study (Figure
30 5). The task is to decide which of two probe items is more neurally similar
31 to the standard stimulus. Trials are defined as correct when the probe that
32 matches in shape is more neurally similar. To foreshadow our results, neural
33 measures that perform best in our decoding analysis perform best in the
34 triplet task, despite the entire classes used in the triplet task being withheld
35 from the decoding analysis. These results indicate that approximating the
36 information available in a brain state through decoding can select similarity
37 measures that broadly generalize and perform sensibly in novel tasks.

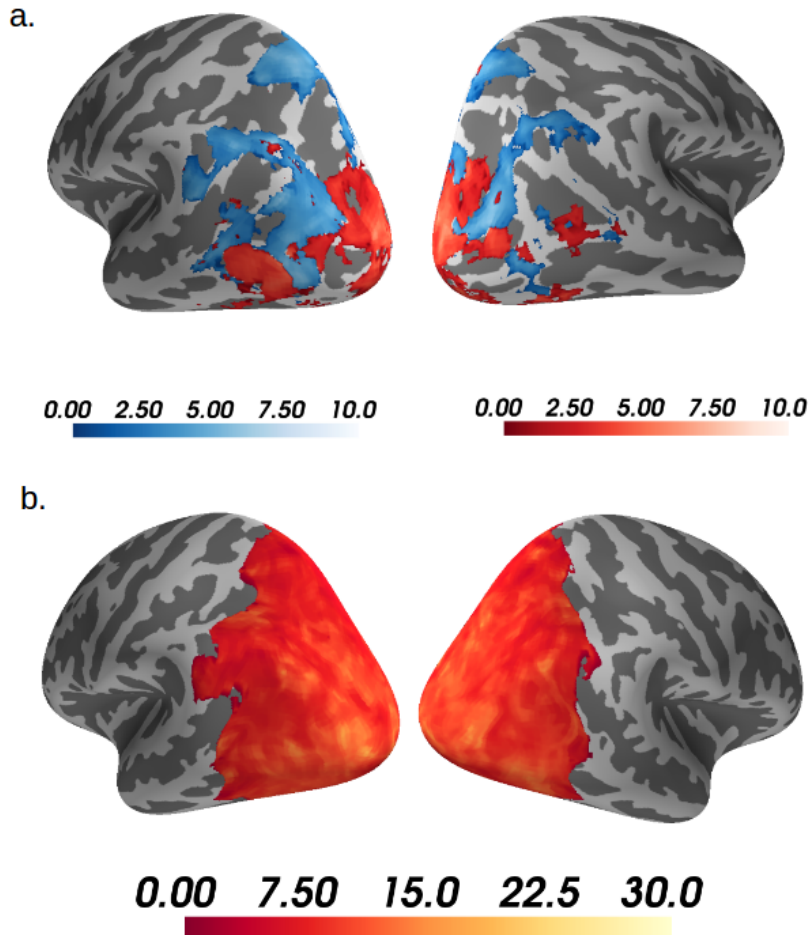


Figure 4: Euclidean & Mahalanobis(r) outperform Pearson. Occipito-lateral views of the left and right hemispheres for the GS study (a) and the NI study (b) displaying maximum t statistics where either the Euclidean measure (blue) or the Mahalanobis(r) measure (red) outperformed the Pearson correlation measure (i.e., each voxel displays the t statistic for the measure with highest t). The t statistics were based on a searchlight analysis of Spearman correlations of each measure with each voxel's SVM confusion matrix (see Materials and Methods). Only displaying t statistics where $p < 0.001$ for paired sample t -tests, TFCE corrected; computed with FSL's randomise function with 5000 permutations, using as a mask the 12 ROIs with best accuracy (see Materials and Methods). Note: very few voxels only show the Euclidean measure significantly outperforming Pearson correlation in the NI study, thus do not appear in this visualization.

1 The triplet task allows a separate evaluation of the similarity measures of
2 interest by comparing the accuracies in such a task to the similarity profile
3 of the NI Study (Figure 5a); Pearson correlation of $r(12) = 0.63, p = 0.017$,
4 across the fourteen similarity measures of interest. For this association, the
5 scatterplot in Figure 5a shows the variance associated to the twelve regions
6 of interest presented above. Measures like Mahalanobis and Mahalanobis(r)
7 clearly do best; in line with the original similarity profile of the NI Study
8 reported in the Neural Similarity analysis (Figure 3a). The similarity profile
9 correlations were adjusted to account for the held-out pairs from the triplet
10 task (with standard and correct probe removed), thus termed (*reduced*) in
11 contrast to the original profile and reported here as (*complete*) (see Materials
12 and Methods). In Figure 5b, all the similarity profiles are related amongst
13 each other and with the triplet task accuracies. Most notably, the bottom row
14 of the diagonal matrix displays how the triplet task accuracies also Pearson
15 correlate negatively with the GS Study Similarity profile as in Figure 3d,
16 $r(12) = -0.81, p < 0.001$. For comparison purposes, we also present the
17 Pearson correlation of the triplet task accuracies with NI Study Similarity
18 profile (*complete*), $r(12) = 0.63, p = 0.016$. The triplet task is thus an
19 independent assessment of the validity of our neural similarity analysis.

20 These results clearly demonstrate that there is no circularity in our method
21 of selecting similarity measures based on a decoding approach that approxi-
22 mates the information available in a brain state. In the triplet task, similarity
23 measures that performed best in our neural similarity analysis also performed
24 best in this novel task involving untrained classes.

25 More basic evidence against circularity claims is also presented in the SI;
26 the best-performing classifier is a linear SVM for both the GS and NI study
27 whereas we find dramatic differences in similarity profiles between studies.
28 Clearly, similarity is not a simple recapitalization of classification.

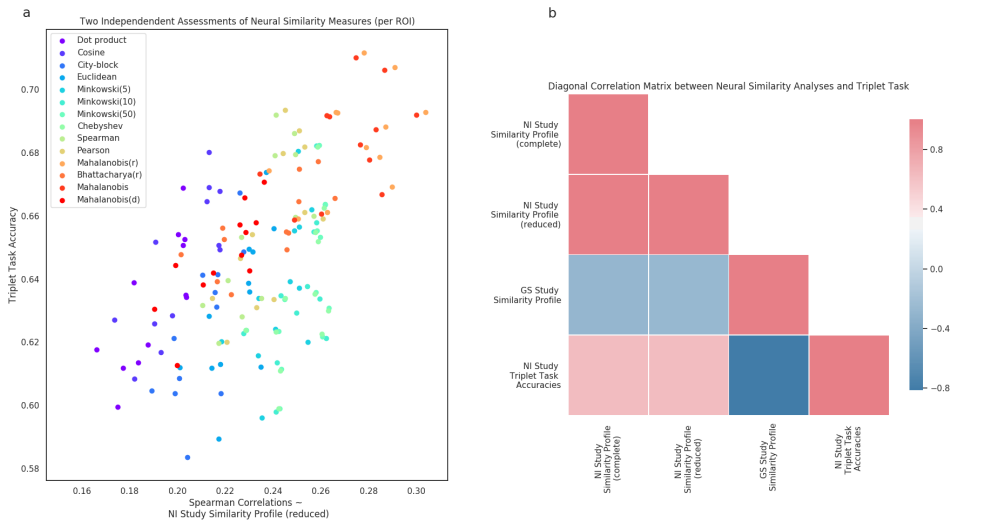


Figure 5: Triplet task accuracies correlate with NI Study similarity profiles. In (a) each data point represents one similarity measure per region of interest. The Spearman correlations in (a) have been recalculated with the removal of held-out pairs used in the triplet task (where each pair is the standard and the correct probe), thus termed NI Study similarity profile (reduced) (see Materials and Methods). In (b) we Pearson correlate the similarity profiles from the Neural Similarity analysis with the accuracies derived from the triplet task as well as with each other. NI Study similarity profile (complete) and GS Study similarity profile are the same Spearman correlations as displayed in Figure 3a (see Materials and Methods).

1 3. Discussion

2 One fundamental question for neuroscience is what makes two brain states
3 similar. This question is so basic that in some ways it has been overlooked
4 or sidestepped by assuming that Pearson correlation captures neural similar-
5 ity. Here, we made an initial effort to evaluate empirically which of several
6 competing similarity measures is the best description of neural similarity.

7 Our basic approach was to characterize the question as a model selec-
8 tion problem in which each similarity measure is a competing model. The
9 various similarity measures (i.e., models) competed to best account for the
10 data, which was the confusion matrix from a classifier (i.e., decoder) that
11 approximated the information present in a brain region of interest. The mo-
12 tivation for this approach is that more similar items (e.g., a sparrow and a
13 robin) should be more confusable than dissimilar items (e.g., a sparrow and a
14 moped). Thus, the test of a similarity measure, which is a pairwise operator
15 on two neural representations, is how well its predicted neural similarities
16 agree with the classifier's confusion matrix.

17 At this early juncture, basic questions, such as whether different brain
18 regions use different measures of similarity and whether the nature of neural
19 similarity is constant across studies remained unanswered. Our results indi-
20 cated that the neural similarity profile (i.e., the pattern of performance across
21 candidate similarity measures) was constant across brain regions within a
22 study, though strongly differed across the two studies we considered. Fur-
23 thermore, Pearson correlation, the *de facto* standard for neural similarity,
24 was bested by competing similarity measures in both studies.

25 Support for the validity of our method came from the follow-on triplet
26 task in which we tested the ability of the similarity measures to select which
27 of two probe items was most neurally similar to a comparison item. Simi-
28 larity measures that performed best at this task (by selecting the probe that
29 matched the comparison in stimulus shape) were those that also performed
30 best under our decoding approach to evaluating neural similarity, despite
31 the fact that the stimuli and classes used in the triplet were withheld from
32 the decoding analyses. These results establish that our method of evaluat-
33 ing similarity measures selects measures that generalize well to novel tasks
34 and stimulus classes. It also highlights that similarity and classification are
35 distinct functions.

36 Accordingly, we report results in the SI in which the best performing
37 similarity measures vary while the best performing classifier remains con-

1 stant, providing an illustration of how similarity and classifier performance
2 can diverge. Of course, despite similarity and classification being distinct,
3 the classifier used to estimate the information present in a brain region could
4 bias the results. We recommend the procedure we followed: Consider a va-
5 riety of classifiers and choose the best performing classifier independently of
6 how the neural similarity measures perform (see SI). In practice, this means
7 that an advance in classifier techniques would invite reconsidering how neural
8 similarity measures perform.

9 One question is why the neural similarity profile would differ across stud-
10 ies. There are host of possibilities. One is that the nature of stimuli drove
11 the differences. The stimuli in the GS study were designed to be psycho-
12 logically separable, consisting of four independent binary dimensions (color:
13 red or green, shape: circle or triangle, size: large or small, and position:
14 right or left). These stimuli were designed to conform to a Euclidean space
15 so that cognitive models assuming such similarity spaces could be fit to the
16 behavioural data. Accordingly, in our analyses, the neural similarity mea-
17 sures from the Minkowski family (including Euclidean) performed best. In
18 contrast, the NI study consisted of naturalistic stimuli (photographs) that
19 covaried in a manner not easily decomposable into a small set of shared fea-
20 tures. One possibility is that these types of complex feature distributions are
21 better paired with the Mahalanobis measure (cf. [48]). Of course, task also
22 varied with stimuli which offers yet another possible higher-level explanation
23 for the differences observed in neural similarity performance. For example,
24 the task in the GS study emphasized analytically decomposing stimuli into
25 separable dimensions whereas holistic processing of differences was a viable
26 strategy in the NI study. In general, different tasks will require neural rep-
27 resentations that differ in their dimensionality or complexity [26], which has
28 ramifications for what similarity measure is most suitable.

29 A host of other concerns related to data quality may also influence how
30 similarity measures perform. The nature of fMRI BOLD response itself places
31 strong constraints on the types of models that can succeed [49], which sug-
32 gests that future work should apply the techniques presented here to other
33 measures of neural activity. Regardless of the measure of neural activity,
34 more complex models of neural similarity will require higher quality data
35 to be properly estimated. For example, measures such as Mahalanobis or
36 Bhattacharyya need to estimate inverse covariance matrices. These matrices
37 grow with the square of the number of vector components which approaches
38 both numerical and statistical unreliability when the number of components

1 approaches the number of observations. For these reasons, we optimized the
2 number of top features (i.e., voxels) separately for each similarity measure
3 (see Materials and Methods), except in the searchlight analysis where this
4 was not possible. We also considered regularized versions of similarity mea-
5 sures, such as Mahalanobis(d), that should be more competitive when data
6 quality is limited.

7 Although the similarity measures considered are relatively simple, they
8 make a host of assumptions that are theoretically and practically conse-
9 quential. For example, angle measures, such as Pearson correlation, are
10 unconcerned with differences in the overall level of neural activity, an as-
11 sumption that strongly contrasts with magnitude measures, such as those
12 in the Minkowski family (e.g., Euclidean measure). Therefore, the choice
13 of similarity measure is central to any mechanistic theory of brain function
14 and has practical ramifications when analyzing neural data, such as when
15 characterizing neural representation spaces. In this light, operations that
16 may seem routine, such as normalizing data in various ways, can affect the
17 interpretation of results. For example, vector cosine only differs from dot
18 product by virtue of normalizing by the magnitude of the two state vectors.

19 As mentioned previously, the space of possible similarity measures is un-
20 countably infinite and new measures routinely enter the literature [50, 46]. In
21 line with our main results, sometimes new measures like crossnobis perform
22 well, and sometimes they fail [51]. Here, we aimed to include representative
23 measures from the main families of similarity measures we identified (see
24 Figure 1, left side). Others are free to replicate our analyses with alternative
25 sets of measures.

26 Although we focus on the BOLD response, our approach applies equally
27 to other neural measures, such as single-unit recordings. One important open
28 question is whether the same similarity measures perform well across mea-
29 sures that differ dramatically in terms of spatial and temporal resolution, as
30 well as the aspects of neural activity they capture. Likewise, our approach
31 can be applied to complex artificial neural networks, such as deep convolu-
32 tions neural networks (CNN), which have become popular in neuroscience by
33 virtue of their ability to track neural activity along the ventral stream during
34 object recognition tasks [52]. In standard neural networks, the basic math-
35 ematics of integrate-and-fire artificial neurons (i.e., units) can be viewed as
36 a similarity operation, namely a dot product between the weight representa-
37 tion of the unit and the activity pattern at the previous layer. Alternatively,
38 many of the other similarity functions we considered are differentiable and

1 could be used in CNNs trained through backpropagation to perhaps provide
2 better performance and agreement with neural measures. The question of
3 which similarity functions manifest at the unit level of a CNN vs. at a larger
4 organizational level recapitulate the previous discussion of the human brain.

5 In conclusion, we took a step toward determining what makes two brain
6 states similar. Working with two fMRI datasets, we found that the best
7 performing similarity measures are common across brain regions within a
8 study, but vary across studies. Furthermore, we found that the *de facto* sim-
9 ilarity measure, Pearson correlation, was bested in both studies. Although
10 follow-up work is needed, the current findings and technique suggest a host
11 of productive questions and have practical ramifications, such as determining
12 the appropriate measure of similarity before conducting a neural repres-
13 entational analysis. In time, efforts making use of this and similar approaches
14 may lead to mechanistic theories that bridge neural circuits, related mea-
15 surement data, and higher-level descriptions.

16 4. Materials and Methods

17 4.1. Datasets

18 The analyses are based on two previous fMRI studies: a study that pre-
19 sented simple geometric shapes (GS) to participants [28] and a study that
20 presented natural images (NI) to participants [6]. The GS study consisted
21 of a visual categorization task with 20 participants and the NI study of a 1-
22 back size judgment task with 14 participants. Descriptions of the tasks and
23 acquisition parameters can be consulted in the SI. For further information,
24 the reader should consult the source citation directly.

25 4.2. Classification analysis

26 Pattern classification analyses were implemented using PyMVPA [53],
27 Scikit-Learn [54], and custom Python code. The input to the classifiers
28 were least squares separate (LS-S) beta coefficients for each presentation of a
29 stimulus [55] (see SI). Three classifiers were used for the pattern classification:
30 Gaussian naïve Bayes, k -nearest neighbor, and linear support vector machine
31 (SVM). The output of one of these classifiers was to be chosen as the best
32 representation of the underlying similarity matrix to which all other similarity
33 measures would be compared to (see Neural similarity analysis below). The
34 linear SVM was implemented with the Nu parametrization [56]. This Nu
35 parameter controls the fraction of data points inside the soft margin; the

1 default value of 0.5 was used for all classifications. The k -nearest neighbor
2 classifier was implemented using five neighbors. No hyperparameters required
3 setting for the Gaussian naïve Bayes classifier.

4 To pick the best-performing classifier, classification was conducted on
5 the whole-brain (no parcellation into distinct ROIs) for each study indepen-
6 dently. All classifiers were trained with leave-one-out k -fold cross-validation,
7 where k was equal to the number of functional runs for each participant in
8 each study (e.g. six runs in the GS study or sixteen runs in the NI study).
9 To do feature selection on voxels, all voxels were ordered according to their
10 F values computed from an ANOVA across all class (stimuli) labels. The
11 top 300 voxels with the highest F values were retained based on classifier
12 performance (i.e., accuracy) on the test run. For these classifiers, accuracy
13 was computed across all classes (16 classes for the GS study and 54 classes for
14 the NI study) with a majority vote rule across all computed decision bound-
15 aries (for classifiers where this is applicable like linear SVM). This means
16 that random classification is equal to 6.25% for the GS study and 1.85% for
17 the NI study for this whole-brain analysis. However, for all other classifi-
18 cation analyses, accuracy is computed as mean pairwise accuracy across all
19 classes, which means that random classification is equal to 50%. The best-
20 performing classifier was selected as the classifier with highest mean accuracy
21 (mean across participants) in the GS and NI study, independently. Classi-
22 fier accuracies (i.e., confusion matrices) were multiplied by negative one for
23 the neural similarity analysis explained. This was done so that they would
24 correlate positively with the similarity measures and facilitate presentation
25 of results.

26 The following analysis was performed for each of the 110 ROIs that are de-
27 scribed in the SI. To train the classifiers leave-one-out k -fold cross-validation
28 was also used. Within each fold, a (randomly) picked validation run was
29 used to tune the number of features (i.e., voxels) that would be selected for
30 that fold. Thus, feature selection was done within each fold. To do this fea-
31 ture selection, all voxels were ordered according to their F values computed
32 from an ANOVA across all class (stimuli) labels. This step aids classifier
33 performance because it preselects task relevant voxels (as opposed to item
34 discriminative voxels). It is important to note that these ANOVAs were com-
35 puted on the training runs but not on the validation run nor on the held-out
36 test run, to avoid overfitting. The top n voxels with the highest F values
37 were retained based on classifier performance (i.e., accuracy) on the valida-
38 tion run. Scipy's *minimize_scalar* function [57] was used to optimize this

1 validation run accuracy with respect to the top n voxels. After picking the
2 top n voxels, the classifiers were trained on both the training runs and the
3 validation run. Subsequently, the classifiers were tested on the held-out test
4 run for that fold. This classification analysis was done for all possible pair-
5 wise classifications for each study (i.e., 120 pairwise classifications in the GS
6 study and 1431 pairwise classifications in the NI study). From this analysis,
7 the pairwise classification accuracies were retained for both the validation
8 run and the test run for each fold. Further ROI selection (top twelve ROIs
9 reported in the Results) is described in the SI.

10 *4.3. Neural similarity analysis*

11 The goal of this analysis was to compare the representation of different
12 similarity measures in the brain. The regions considered here are the ones
13 reported in the Results and described in the secondary ROI selection sec-
14 tion in the SI. The comparison criterion was chosen as Spearman correlation
15 between all pairwise similarities and the classification accuracies mentioned
16 above. This criterion was used since it avoids scaling issues. To achieve this,
17 first all pairwise similarities (i.e., for all pairs of stimuli) were computed from
18 the training runs defined in the classification analysis not including the vali-
19 dation run. Incidentally, feature selection was also realized here. In the same
20 fashion as in the classification analysis, all voxels were ordered according to
21 their F values computed from an ANOVA across all class (stimuli) labels.
22 Then, the top n voxels with the highest F values were retained based on
23 Spearman correlation of the similarities with the validation run accuracies of
24 the classifier that were previously computed. After picking the top n voxels,
25 the similarities were computed across training runs and validation run for
26 those voxels. These similarities were then used to compute the final Spear-
27 man correlation with the classifier test run accuracies. Conducting feature
28 selection for the similarity measures is important because different measures
29 leverage information differently.

30 This analysis parallels the classification analysis in every way except that
31 instead of optimizing model accuracy, here the optimization criterion was
32 model correlation (i.e., Spearman correlation) with the previously computed
33 pairwise classifier accuracies.

34 *4.4. Mixed effects models*

35 A mixed effects model was performed with the lme4 package [58] for
36 each study with Spearman correlations from the neural similarity analysis

1 (i.e., similarity profile) as the response variable. The models contained fixed
2 effects of similarity measure, linear SVM accuracy, participant, and ROI.
3 Linear SVM accuracy, participant, and ROI variables only serve to account
4 for variance and obtain better estimates. The models also contained random
5 effects of ROI (varying per participant) and of similarity measure (varying
6 per ROI). Model comparisons were performed between the full model and a
7 null model without any similarity measures.²

8 *4.5. Post hoc searchlight analysis*

9 Searchlight analyses [59] have become an increasingly popular multivari-
10 ate tool for spatial localizations of brain activations in recent years. This
11 analysis is based on the definition of a sphere with radius in millimeters (or
12 cube with radius in number of voxels) that computes a statistic, centered on
13 each voxel of interest, using as input only the voxel values that fall within the
14 confines of the predefined sphere. Depending on the number of voxels con-
15 sidered, this analysis can be computationally expensive. Thus for reasons of
16 computational tractability, a searchlight analysis was not used as the primary
17 analysis but as a *post hoc* tool to inquire over the spatial specificity of cer-
18 tain measures of interest commonly used in the literature such as Euclidean,
19 Pearson correlation and Mahalanobis [16]. Since optimizing the searchlight
20 radius for each voxel is not feasible with current computational resources - to
21 equate measure complexity by feature selection as done in the main analysis
22 - the searchlight radius was set to 3 voxels. The analysis was done only for
23 Euclidean, Pearson correlation, and Mahalanobis(r). This searchlight anal-
24 ysis was done within the union of the top 10 ROIs across both studies (see
25 Secondary ROI selection above) in the native space of each subject using
26 PyMVPA's searchlight function. For each voxel, the similarity matrices were
27 Spearman correlated with the best performing classifier in the same fashion
28 as in the main analysis above. For each study, the statistical maps of Eu-
29 clidean and Mahalanobis(r) were compared to the statistical map of Pearson
30 correlation, using it as a baseline measure. All maps were transformed to
31 MNI space for this comparison. The threshold-free enhancement (TFCE)
32 corrected *p* values for the paired *t* statistics were computed with FSL's ran-
33 domise function with 5000 permutations. Only *t* statistics that presented
34 TFCE corrected *p* values below 0.001 were considered as significant. This

²A full model that included both studies was not possible due to convergence issues.

1 more conservative threshold was based upon this being a *post hoc* analysis
2 (i.e., supposing all 17 measures would have been compared against Pearson
3 correlation, then the appropriate Bonferroni corrected threshold would have
4 been $p = 0.05/17 \approx 0.0029$).

5 *4.6. Triplet task*

6 In this task, a stimulus is chosen as a standard and paired with a correct
7 probe. These pairs of standard and correct probe are designated as held-out
8 pairs for reasons that will seem obvious below. The correct probes are chosen
9 so as to share a common dimension with the standard. For the NI study, this
10 was possible since shape (or silhouette) and category were two orthogonal di-
11 mensions that were part of the experimental setup of the fifty-four stimuli
12 in the original study. In that study, six categories of stimuli were orthogonal
13 to nine types of shape or silhouette (see SI). Subsequently, incorrect probes
14 were chosen on the basis of not sharing values for either the shape or cat-
15 egory dimensions for both the standard and correct probe. Thus, if basing
16 the choice of correct probe on agreement with the shape dimension, then
17 thirty-two (out of fifty-four) stimuli remain as choices for incorrect probes
18 (i.e., shape triplet task). However, if the choice of correct probe is agreement
19 with category, then thirty-five (out of fifty-four) stimuli remain as choices
20 for incorrect probes (i.e., category triplet task). Either way, the task then
21 consists of comparing the similarity between standard and correct probe with
22 similarity between standard and incorrect probe for a given similarity mea-
23 sure. If the similarity measure is higher between standard and correct probe
24 than it is for standard and incorrect probe, then the outcome of such a com-
25 parison is labelled with value one, otherwise zero. This operation was done
26 for all possible incorrect probes and accuracy was computed as the number
27 of outcomes equal to one divided by the number of incorrect probes (thirty-
28 two for the shape triplet task and thirty-five for the category triplet task).
29 This procedure was repeated for all possible pairs of standard and correct
30 probe per similarity measure (out of 14 similarity measures reported in the
31 Results), per run, per region of interest (out of the 12 ROIs reported in the
32 Results), and per subject.

33 Accuracies computed for the triplet task should show performance of
34 similarity measures that are in agreement with the similarity profiles from
35 the neural similarity analysis. To adequately assess such an agreement, we
36 recalculated the similarity profiles based on a subset of the original Spearman
37 correlations used in the neural similarity analysis. The subset consisted of

1 removing correlations for held-out pairs (standard and correct probe) that
2 were being assessed in the triplet task. Such a procedure is necessary to
3 claim independence between the neural similarity analysis and the triplet
4 task and avoid inflated correlations between tasks. This subset of Spearman
5 correlations was used to calculate the similarity profile referred to as *NI*
6 *Study Similarity Profile (reduced)*, whereas the original similarity profile was
7 referred to as *NI Study Similarity Profile (complete)* in the Triplet Task
8 subsection of the Result section.

9 **Data and code availability**

10 For open access to the data or code please visit:
11 1) Raw fMRI data for the GS Study: <https://osf.io/62rgs/>
12 2) Raw fMRI data for the NI Study: <https://osf.io/qp54f/>
13 3) Data and code for the neural similarity analysis: <https://osf.io/5a6bd/>

14 **Acknowledgements**

15 From the Love Lab, we thank Olivia Guest, Kurt Braunlich, Brett Roads,
16 Rob Mok, Adam Hornsby, and Xiaoliang Luo for their comments. We thank
17 the authors of the NI and GS Studies for making their data publicly avail-
18 able. This research was supported by a scholarship from Consejo Nacional de
19 Ciencia y Tecnologa (CONACYT) and an enrichment year stipend from The
20 Alan Turing Institute to SBS and by the NIH Grant 1P01HD080679, Lever-
21 hulme Trust grant RPG-2014-075, and Wellcome Trust Senior Investigator
22 Award WT106931MA to BCL.

23 **Author contributions**

24 BCL developed the study concept. BCL and SBS contributed to the
25 study design. SBS performed the data analysis and interpretation under the
26 supervision of BCL. AM and AP performed confirmatory checks of the results
27 and auxiliary analyses. SBS drafted the manuscript. BCL and CA provided
28 critical revisions. All authors approved the final version of the manuscript
29 for submission.

30 **Competing financial interests**

31 The authors declare no competing financial interests.

1 References

- 2 [1] D. L. Medin, R. L. Goldstone, D. Gentner, Respects for similarity., Psychological review 100 (1993) 254.
- 3 [2] R. L. Goldstone, The role of similarity in categorization: providing a groundwork, Cognition 52 (1994) 125–157.
- 4 [3] A. B. Markman, W. T. Maddox, D. a. Worthy, B. Markman, and Ex-
5 celling Under Choking Pressure, Psychological Science 17 (2006) 944–
6 948.
- 7 [4] M. N. Coutanche, S. L. Thompson-Schill, Creating concepts from con-
8 verging features in human cortex, Cerebral Cortex 25 (2014) 2584–2593.
- 9 [5] T. J. Palmeri, I. Gauthier, Visual object understanding, Nature Reviews
10 Neuroscience 5 (2004) 291.
- 11 [6] S. Bracci, H. O. de Beeck, Dissociations and associations between shape
12 and category representations in the two visual pathways, Journal of
13 Neuroscience 36 (2016) 432–444.
- 14 [7] A. Tversky, Features of similarity., Psychological review 84 (1977) 327.
- 15 [8] D. M. Ennis, J. J. Palen, K. Mullen, A multidimensional stochastic
16 theory of similarity, Journal of Mathematical Psychology 32 (1988)
17 449–465.
- 18 [9] J. B. Tenenbaum, T. L. Griffiths, Generalization, similarity and
19 Bayesian inference, Behavioral and Brain Sciences 24 (2001) 629–640.
- 20 [10] D. Gentner, A. B. Markman, Structure mapping in analogy and simi-
21 larity., American psychologist 52 (1997) 45.
- 22 [11] E. M. Pothos, J. R. Busemeyer, J. S. Trueblood, A quantum geometric
23 model of similarity., Psychological Review 120 (2013) 679.
- 24 [12] U. Hahn, N. Chater, L. B. Richardson, Similarity as transformation,
25 Cognition 87 (2003) 1–32.
- 26 [13] C. L. Krumhansl, Concerning the applicability of geometric models
27 to similarity data: The interrelationship between similarity and spatial
28 density., Psychological Review 85 (1978) 445–463.

1 [14] N. Kriegeskorte, M. Mur, P. Bandettini, Representational similarity
2 analysis - connecting the branches of systems neuroscience., Frontiers
3 in systems neuroscience 2 (2008) 4.

4 [15] G. Xue, Q. Dong, C. Chen, Z. Lu, J. A. Mumford, R. A. Poldrack,
5 Greater neural pattern similarity across repetitions is associated with
6 better memory, Science 330 (2010) 97–101.

7 [16] H. Nili, C. Wingfield, A. Walther, L. Su, W. Marslen-Wilson,
8 N. Kriegeskorte, A Toolbox for Representational Similarity Analysis,
9 PLoS Computational Biology 10 (2014).

10 [17] M. Weber, S. L. Thompson-Schill, D. Osherson, J. Haxby, L. Parsons,
11 Predicting judged similarity of natural categories from their neural rep-
12 resentations, Neuropsychologia 47 (2009) 859–868.

13 [18] K. F. LaRocque, M. E. Smith, V. A. Carr, N. Witthoft, K. Grill-Spector,
14 A. D. Wagner, Global similarity and pattern separation in the human
15 medial temporal lobe predict subsequent memory, Journal of Neuro-
16 science 33 (2013) 5466–5474.

17 [19] T. Davis, R. A. Poldrack, Quantifying the internal structure of cat-
18 egories using a neural typicality measure, Cerebral Cortex 24 (2013)
19 1720–1737.

20 [20] N. Kriegeskorte, M. Mur, D. A. Ruff, R. Kiani, J. Bodurka, H. Esteky,
21 K. Tanaka, P. A. Bandettini, Matching categorical object representa-
22 tions in inferior temporal cortex of man and monkey, Neuron 60 (2008)
23 1126–1141.

24 [21] T. Davis, G. Xue, B. C. Love, A. R. Preston, R. A. Poldrack, Global
25 neural pattern similarity as a common basis for categorization and recog-
26 nition memory, Journal of Neuroscience 34 (2014) 7472–7484.

27 [22] E. R. Soucy, D. F. Albeanu, A. L. Fantana, V. N. Murthy, M. Meister,
28 Precision and diversity in an odor map on the olfactory bulb, Nature
29 neuroscience 12 (2009) 210–220.

30 [23] M. C. W. van Rossum, A novel spike distance, Neural computation 13
31 (2001) 751–763.

1 [24] C. Gardella, O. Marre, T. Mora, Blindfold learning of an accurate
2 neural metric, *Proceedings of the National Academy of Sciences* (2018)
3 201718710.

4 [25] J. Diedrichsen, G. R. Ridgway, K. J. Friston, T. Wiestler, Comparing
5 the similarity and spatial structure of neural representations: A pattern-
6 component model, *NeuroImage* 55 (2011) 1665–1678.

7 [26] C. Ahlheim, B. C. Love, Estimating the functional dimensionality of
8 neural representations, *NeuroImage* (2018).

9 [27] K. Braunlich, B. C. Love, Occipitotemporal Representations Reflect
10 Individual Differences in Conceptual Knowledge, *bioRxiv* (2018).

11 [28] M. L. Mack, A. R. Preston, B. C. Love, Decoding the brain’s algorithm
12 for categorization from its neural implementation, *Current Biology* 23
13 (2013) 2023–2027.

14 [29] M. L. Mack, B. C. Love, A. R. Preston, Dynamic updating of hippocam-
15 pal object representations reflects new conceptual knowledge, *Proceed-
16 ings of the National Academy of Sciences* 113 (2016) 13203–13208.

17 [30] R. Mihalcea, C. Corley, C. Strapparava, others, Corpus-based and
18 knowledge-based measures of text semantic similarity, in: AAAI, vol-
19 ume 6, pp. 775–780.

20 [31] C. Alfeld, J. D. Haynes, Searchlight-based multi-voxel pattern analysis
21 of fMRI by cross-validated MANOVA, *NeuroImage* 89 (2014) 345–357.

22 [32] J. V. Haxby, J. S. Guntupalli, A. C. Connolly, Y. O. Halchenko, B. R.
23 Conroy, M. I. Gobbini, M. Hanke, P. J. Ramadge, A common, high-
24 dimensional model of the representational space in human ventral tem-
25 poral cortex, *Neuron* 72 (2011) 404–416.

26 [33] R. Kiani, H. Esteky, K. Mirpour, K. Tanaka, Object category structure
27 in response patterns of neuronal population in monkey inferior temporal
28 cortex., *Journal of neurophysiology* 97 (2007) 4296–4309.

29 [34] R. M. Nosofsky, Similarity scaling and cognitive process models, *Annual
30 review of Psychology* 43 (1992) 25–53.

1 [35] T. Davis, G. Xue, B. C. Love, A. R. Preston, R. a. Poldrack, Global
2 Neural Pattern Similarity as a Common Basis for Categorization and
3 Recognition Memory, *Journal of Neuroscience* 34 (2014) 7472–7484.

4 [36] D. J. Heeger, Normalization of cell responses in cat striate cortex, *Visual*
5 *neuroscience* 9 (1992) 181–197.

6 [37] R. Brunelli, T. Poggio, Face recognition: Features versus templates,
7 *IEEE transactions on pattern analysis and machine intelligence* 15
8 (1993) 1042–1052.

9 [38] R. N. Shepard, Attention and the metric structure of the stimulus space,
10 *Journal of Mathematical Psychology* 1 (1964) 54–87.

11 [39] K. W. Spence, The nature of the response in discrimination learning.,
12 *Psychological review* 59 (1952) 89.

13 [40] I. P. Pavlov, G. V. Anrep, *Conditioned reflexes*, Courier Corporation,
14 2003.

15 [41] M. Jenkinson, C. F. Beckmann, T. E. J. Behrens, M. W. Woolrich, S. M.
16 Smith, *Fsl*, *Neuroimage* 62 (2012) 782–790.

17 [42] A. Bhandari, C. Gagne, D. Badre, Just above Chance: Is It Harder
18 to Decode Information from Prefrontal Cortex Hemodynamic Activity
19 Patterns?, *Journal of Cognitive Neuroscience* 30 (2018) 1473–1498.

20 [43] M. S. Bartlett, The effect of standardization on a χ^2 approximation in
21 factor analysis, *Biometrika* 38 (1951) 337–344.

22 [44] R. I. Jennrich, An asymptotic χ^2 test for the equality of two correlation
23 matrices, *Journal of the American Statistical Association* 65 (1970)
24 904–912.

25 [45] M. Persson, J. Rieskamp, Inferences from memory: Strategy- and
26 exemplar-based judgment models compared, *Acta Psychologica* 130
27 (2009) 25–37.

28 [46] A. Walther, H. Nili, N. Ejaz, A. Alink, N. Kriegeskorte, J. Diedrichsen,
29 Reliability of dissimilarity measures for multi-voxel pattern analysis,
30 *NeuroImage* 137 (2016) 188–200.

1 [47] V. Fritsch, G. Varoquaux, B. Thirion, J.-B. Poline, B. Thirion, Detecting outliers in high-dimensional neuroimaging datasets with robust
2 covariance estimators, *Medical image analysis* 16 (2012) 1359–1370.

3

4 [48] J. Diedrichsen, N. Kriegeskorte, Representational models: A common
5 framework for understanding encoding, pattern-component, and
6 representational-similarity analysis, 2016.

7 [49] O. Guest, B. C. Love, What the success of brain imaging implies about
8 the neural code, *Elife* 6 (2017) e21397.

9 [50] C. Aliefeld, J.-D. Haynes, Searchlight-based multi-voxel pattern analysis
10 of fMRI by cross-validated MANOVA, *Neuroimage* 89 (2014) 345–357.

11 [51] I. Charest, N. Kriegeskorte, K. N. Kay, GLMdenoise improves multi-
12 variate pattern analysis of fMRI data, *NeuroImage* 183 (2018) 606–616.

13 [52] D. L. K. Yamins, J. J. DiCarlo, Using goal-driven deep learning models
14 to understand sensory cortex, *Nature neuroscience* 19 (2016) 356.

15 [53] M. Hanke, Y. O. Halchenko, P. B. Sederberg, S. J. Hanson, J. V. Haxby,
16 S. Pollmann, PyMVPA: a python toolbox for multivariate pattern analysis
17 of fMRI data, *Neuroinformatics* 7 (2009) 37–53.

18 [54] F. Pedregosa, G. Varoquaux, A. Gramfort, V. Michel, B. Thirion,
19 O. Grisel, M. Blondel, P. Prettenhofer, R. Weiss, V. Dubourg, Scikit-
20 learn: Machine learning in Python, *Journal of Machine Learning Research* 12 (2011) 2825–2830.

21

22 [55] J. A. Mumford, B. O. Turner, F. G. Ashby, R. A. Poldrack, Deconvolving BOLD activation in event-related designs for multivoxel pattern
23 classification analyses, *Neuroimage* 59 (2012) 2636–2643.

24

25 [56] B. Schölkopf, A. J. Smola, R. C. Williamson, P. L. Bartlett, New support
26 vector algorithms, *Neural computation* 12 (2000) 1207–1245.

27 [57] T. E. Oliphant, SciPy: Open source scientific tools for Python, 2007.

28 [58] D. Bates, M. Maechler, B. Bolker, S. Walker, lme4: Linear mixed-effects
29 models using Eigen and S4, *R package version* 1 (2014) 1–23.

1 [59] N. Kriegeskorte, R. Goebel, P. Bandettini, Information-based functional
2 brain mapping, Proceedings of the National Academy of Sciences of the
3 United States of America 103 (2006) 3863–3868.

Supplementary Information

1 1. Task descriptions and fMRI parameters

2 2. A.1 Geometric shapes (GS) study

3 3 The GS study presented sixteen objects in total, which varied on four
4 4 different binary features: (color: red or green, shape: circle or triangle, size:
5 5 large or small, and position: right or left). Participants in this study were
6 6 trained to do a categorization task. They were first trained on five objects of
7 7 one category and four of the other (nine objects total during training) with
8 8 twenty repetitions of each object. During the anatomical scan, participants
9 9 saw four more repetitions of the training items as a refresher. Then during
10 10 the functional scanning phase, participants were asked to categorize the nine
11 11 familiar objects they saw during the training phase and seven novel objects
12 12 they had not seen before. Each trial during the functional scanning phase
13 13 lasted 10 seconds; 3.5 seconds where one of the sixteen objects (nine training
14 14 stimuli and seven novel transfer stimuli) was presented after which a fixation
15 15 cross was presented for 6.5 seconds. No feedback was provided during this
16 16 phase. Each stimulus was presented three times within a run across six runs
17 17 resulting in each stimulus being presented a total of eighteen times during the
18 18 functional scanning phase except for one participant who only participated
19 19 in five runs of the scanning phase.

20 20 Whole-brain imaging data were acquired on a 3.0T GE Sigma MRI system
21 21 (GE Medical Systems). Structural images were acquired using a T2-weighted
22 22 flow-compensated spin-echo pulse sequence (TR=3s; TE=68ms, 256x256 ma-
23 23 trix, 1x1mm in-plane resolution) with thirty-three 3-mm thick oblique axial
24 24 slices (0.6mm gap), approximately 20 off the AC-PC line. Functional images
25 25 were acquired with an echo planar imaging sequence using the same slice
26 26 prescription as the structural images (TR=2s, TE=30.5ms, flip angle=73,
27 27 64x64 matrix, 3.75x3.75 in-plane resolution, bottom-up interleaved acqui-
28 28 sition, 0.6mm gap). An additional high-resolution T1-weighted 3D SPGR
29 29 structural volume (256x256x172 matrix, 1x1x1.3mm voxels) was acquired
30 30 for registration and cortex parcellation.

1 *A.2 Natural images (NI) study*

2 The NI study presented fifty-four objects in total, which varied in two
3 ways. The 54 stimulus items were conceived to either be organized by cat-
4 egory (6 categories: minerals, animals, fruits/vegetables, music, sports, or
5 tools) or by their silhouette (9 silhouettes) which cut orthogonally across the
6 category distinction. Participants in this study were asked to perform a 1-
7 back real-world size judgment task (i.e., to respond according to whether the
8 object on the previous trial was larger or smaller than the current image on
9 screen). Participants were scanned on two separate sessions (different days).
10 Each session consisted of eight functional scanning runs resulting in sixteen
11 runs total except for one participant for which four of the runs of the first ses-
12 sion were lost due to scanning issues. Each one of the fifty-four objects were
13 presented twice within each run in a randomized sequence. This resulted in
14 each object being presented a total of thirty-two times (or twenty-four times
15 for the participant that only had twelve runs). On each trial, each object
16 was presented for 1.5 seconds after which a fixation cross was presented for
17 1.5 seconds. Each run started with a fixation cross for fourteen seconds and
18 ended with a fixation cross for fourteen seconds. Thirty-six fixation trials
19 lasting three seconds each were also randomly presented within each run.

20 Data collection was performed on a 3T Philips scanner with a 32-channel
21 coil at the Department of Radiology of the University Hospitals Leuven.
22 MRI volumes were collected using echo planar (EPI) T2*-weighted scans.
23 Acquisition parameters were as follows: repetition time (TR) of 2 s, echo time
24 (TE) of 30 ms, flip angle (FA) of 90°, field of view (FoV) of 216 mm, and matrix
25 size of 72x72. Each volume comprised 37 axial slices (covering the whole
26 brain) with 3 mm thickness and no gap. The T1-weighted anatomical images
27 were acquired with an MP-RAGE sequence, with 1x1x1 mm resolution.

28 *A.3 fMRI preprocessing*

29 The original raw (NIfTI formatted) files from both studies were prepro-
30 cessed and analyzed using FSL 4.1 [1]. Functional images were realigned to
31 the first volume in the time series to correct for motion, co-registered to the
32 T2-weighted structural volume, high-pass filtered (128s), and detrended to
33 remove linear trends within each run. All analyses were performed in the
34 native space of each participant.

1 *A.4 Trial-by-trial estimates*

2 For both studies, after preprocessing the fMRI data with FSL, the method
3 suggested by Mumford et al. [2] known as LS-S (least squares separate) beta
4 estimation was used to get a coefficient estimate for each individual presen-
5 tation of each object. This method consists of calculating a general linear
6 model for each object presentation with only two regressors; one regressor
7 representing the effect of interest (the object presentation in question) and
8 another regressor representing all other object presentations within the re-
9 spective run. This procedure was done for each run separately to preserve
10 as much statistical independence as possible between runs. Such a step is
11 necessary for doing the multivoxel pattern analysis. After successfully esti-
12 mating the object presentation coefficients within each run, these were then
13 concatenated into a single 4D NIfTI formatted file. Furthermore, all runs
14 were subsequently aligned to the last run within each study (e.g. the sixth
15 run in the GS study or the sixteenth run in the NI study). The runs were
16 then concatenated into a single 4D NIfTI formatted file for each participant
17 within each study.

18 *B. Regions of interest from the Harvard-Oxford atlas*

19 *B.1 Initial region of interest (ROI) selection*

20 The Harvard-Oxford cortical and subcortical structural atlases provided
21 with FSL [1] were used to parcellate the different anatomical regions for
22 each participant. A total of 110 regions of interest were used as masks that
23 would be used in the multivoxel pattern analyses. The goal was to evaluate
24 classifier accuracy across the whole brain (except for areas like cerebral white
25 matter or the lateral ventricles). More areas could have been excluded based
26 on a priori hypotheses of where similarity signals would arise. However,
27 including areas where no signal was expected served as an informal control
28 for the method and still retained the possibility that similarity signals could
29 have been found in otherwise unexpected brain regions. The masks were
30 transformed from MNI space to each participants native space. This masking
31 by anatomical region can be considered the first part of a feature selection
32 procedure. Feature selection was also done within each region of interest for
33 each participant (see Materials and Methods). All regions from the Harvard-
34 Oxford atlas were included in the analyses except for cerebral white matter,
35 the lateral ventricles, left and right cerebral cortex, and the brain stem.
36 This results in 48 cortical regions and 7 subcortical regions; doubling for
37 lateralization results in the 110 regions of interest.

1 *B.2 Cortical regions of interest*

2 Frontal Pole, Insular Cortex, Superior Frontal Gyrus, Middle Frontal
3 Gyrus, Inferior Frontal Gyrus (pars triangularis), Inferior Frontal Gyrus (pars
4 opercularis), Precentral Gyrus, Temporal Pole, Superior Temporal Gyrus
5 (anterior division), Superior Temporal Gyrus (posterior division), Middle
6 Temporal Gyrus (anterior division), Middle Temporal Gyrus (posterior di-
7 vision), Middle Temporal Gyrus (temporooccipital part), Inferior Tempo-
8 ral Gyrus (anterior division), Inferior Temporal Gyrus (posterior division),
9 Inferior Temporal Gyrus (temporooccipital part), Postcentral Gyrus, Su-
10 prior Parietal Lobule, Supramarginal Gyrus (anterior division), Supramarginal
11 Gyrus (posterior division), Angular Gyrus, Lateral Occipital Cortex (su-
12 prior division), Lateral Occipital Cortex (inferior division), Intracalcarine Cor-
13 tex, Frontal Medial Cortex, Juxtapositional Lobule Cortex (formerly Supple-
14 mentary Motor Cortex), Subcallosal Cortex, Paracingulate Gyrus, Cingulate
15 Gyrus (anterior division), Cingulate Gyrus (posterior division), Precuneous
16 Cortex, Cuneal Cortex, Frontal Orbital Cortex, Parahippocampal Gyrus (an-
17 terior division), Parahippocampal Gyrus (posterior division), Lingual Gyrus,
18 Temporal Fusiform Cortex (anterior division), Temporal Fusiform Cortex
19 (posterior division), Temporal Occipital Fusiform Cortex, Occipital Fusiform
20 Gyrus, Frontal Operculum Cortex, Central Opercular Cortex, Parietal Oper-
21 culum Cortex, Planum Polare, Heschl's Gyrus (includes H1 and H2), Planum
22 Temporale, Supracalcarine Cortex, & Occipital Pole.

23 *B.3 Subcortical regions of interest*

24 Thalamus, Caudate, Putamen, Pallidum, Hippocampus, Amygdala, &
25 Accumbens.

26 *B.4 Secondary ROI selection*

27 The 110 ROIs were rank ordered by mean classifier accuracy (mean across
28 participants) within each study. Subsequently, the union of the top ten ROIs
29 was selected for the neural similarity analysis. This procedure was done to
30 ensure that the ROIs used to evaluate the similarity measures was based on
31 brain areas with adequate signal-to-noise ratio. The 12 ROIs as reported in
32 the Results were left and right intracalcarine cortex (CALC), left and right
33 lateral occipital cortex (LO) inferior and superior divisions, left and right
34 lingual gyrus (LING), left and right occipital fusiform gyrus (OF), and left
35 and right occipital pole (OP).

1 *C. Classifier selection*

2 The best performing classifier was chosen out of three candidates; Gaussian naïve Bayes (GNB), k -nearest neighbor (KNN), and linear support vector machine (SVM). These classifiers were chosen because they are commonly used in data analysis, both inside and outside the field of neuroimaging, and they compute classification in very distinct ways (see [3]).

7 The linear SVM classifier was the clear winner across both studies, thus was chosen as our gold standard approximation to the brain's similarity measure. The performance of the linear SVM classifier compared to the other 10 two classifiers is shown in Table C1.

	GS Study		NI study	
	mean	s.d.	mean	s.d.
Linear SVM	20.49%	12.64%	23.51%	5.50%
GNB	15.00%	8.79%	10.24%	2.84%
KNN	14.51%	8.50%	8.49%	3.09%
Random classification		6.25%		1.85%
	<i>t</i>	<i>p</i>	<i>t</i>	<i>p</i>
Linear SVM vs. GNB	5.22	< 0.001	14.33	< 0.001
Linear SVM vs. KNN	4.59	< 0.001	17.80	< 0.001
degrees of freedom		19		13

Table C1. Linear SVM is best-performing classifier in both studies. Top panel shows mean accuracy and standard deviations (s.d.) (across participants) for each classifier. Bottom panel shows *t*-tests comparing the best-performing classifier (linear SVM) to the other two classifiers.

11 In addition to comparing the performance of the classifiers judged by 12 their performance accuracy, the confusion matrices between classifiers - from 13 the same analysis - were also compared. Although the classifiers are quite 14 distinct algorithmically speaking, extreme differences between their confu- 15 sion matrices would be unlikely. Indeed it was the case that the average 16 correlations (averaged across subjects) were all significantly above zero for 17 both studies. In the GS study, linear SVM correlated highest with GNB (m 18 = 0.47, s.d. = 0.172, $t(19) = 12.01$, $p < 0.001$), second highest with KNN 19 (m = 0.37, s.d. = 0.197, $t(19) = 8.21$, $p < 0.001$), and GNB correlated 20 with KNN in third place (m = 0.32, s.d. = 0.195, $t(19) = 7.06$, $p < 0.001$).

1 In the NI study, linear SVM correlated highest with GNB (m = 0.35, s.d.
2 = 0.072, $t(13) = 17.55$, $p < 0.001$), second highest with KNN (m = 0.29,
3 s.d. = 0.080, $t(13) = 13.06$, $p < 0.001$), and GNB correlated with KNN in
4 third place (m = 0.22, s.d. = 0.091, $t(13) = 8.94$, $p < 0.001$). These results
5 provide supplementary support for choosing linear SVM as the brain's gold
6 standard for these two datasets given that it's confusion matrix correlates
7 highest with the confusion matrices of the other two classifiers.

8 Thus, the linear SVM classifier was optimized for each of the initial 110
9 ROIs. The ROIs were rank-ordered in terms of accuracy in each study and the
10 union of the top 10 ROIs across both studies was: left and right intracalcarine
11 cortex (CALC), left and right lateral occipital cortex (LO) inferior division,
12 left and right lateral occipital cortex (LO) superior division, left and right
13 lingual gyrus (LING), left and right occipital fusiform gyrus (OF), and left
14 and right occipital pole (OP). This resulted in a secondary ROI selection of
15 12 ROIs with best (linear SVM) classifier accuracy.

16 Classifications were performed pairwise for this analysis and thus random
17 classification was expected at 50% for both studies (see Materials and Meth-
18 ods). The mean accuracy for the linear SVM classifier in the 12 regions of
19 interest was 59.47% (s.d. = 7.97%) in the GS study and 78.43% (s.d. =
20 7.41%) in the NI study. The best-performing classifier (linear SVM) was
21 performing above 50% chance level in both studies; $t(19) = 5.18$, $p < 0.001$,
22 in the GS study and $t(13) = 13.84$, $p < 0.001$, in the NI study (degrees of
23 freedom are based on number of participants for each study). This provides
24 reassurance that the ROIs that were selected indeed have information regard-
25 ing stimuli presentation. Classification accuracy for the NI study was higher
26 than in the GS study $t(32) = 6.82$, $p < 0.001$, showing a potential difference
27 in data quality due to the higher number of observations per stimuli in the
28 NI study (see Materials and Methods).

29 *D. Similarity measures*

30 The following similarity measures were evaluated: dot product, cosine dis-
31 tance, city-block (Manhattan), Euclidean, three variants of Minkowski (with
32 norms 5, 10 and 50), Chebyshev, Spearman correlation, Pearson correlation,
33 three variants of Mahalanobis, three variants of Bhattacharyya, variation
34 of information, and distance correlation. City-block, Euclidean, Minkowski,
35 Chebyshev, Mahalanobis, Bhattacharyya and variation of information are
36 proper distance metrics; to convert them to similarity measures they were
37 multiplied by minus one. Other linking functions between similarities and

1 distances are possible, as in a negative exponential [4], but not relevant here
2 since our optimization criterion was Spearman correlation. The three vari-
3 ants of Mahalanobis and Bhattacharyya were due to the way the sample co-
4 variance matrix was regularized; either no regularization, Ledoit-Wolf shrink-
5 age (implemented through Scikit-Learn, [5, 6] or diagonal regularization. Di-
6 agonal regularization was defined as the sample covariance matrix with all
7 the off-diagonal elements set to zero (see below); such a measure is also
8 known as the normed Euclidean distance. Note that city-block, Euclidean,
9 and Chebyshev are also special cases of the Minkowski measure where the
10 norms are set to one, two and infinity, respectively. To keep calculations con-
11 sistent across all similarity measures, vector representations for each stimulus
12 were defined as the mean vectors across trial presentations for that stimu-
13 lus. Below are the equations for each similarity measure and the covariance
14 matrix regularization procedures.

15 In constructing the similarity profiles, we only used similarity measures
16 that presented a mean Spearman correlation within three median absolute
17 deviations away from the group average (group refers to measures here). Mea-
18 sures that did not meet these criteria were considered outliers (these measures
19 were close to zero mean Spearman correlation). The median Spearman cor-
20 relation across the 18 similarity measures evaluated was 0.203 for the GS
21 study 0.125 and for the NI study and their median absolute deviation was
22 0.0482 for the GS study and 0.0234 for the NI study. The mean Spearman
23 correlations (across participants) and the standard deviations for the mea-
24 sures that were more than three median absolute deviations away from the
25 group average were: Bhattacharya without covariance matrix regularization
26 (mean = 0.001 and s.d. = 0.004 for the GS study, mean = 0.0002 and s.d.
27 = 0.0006 for the NI study), Bhattacharya (d) (with diagonal regularization)
28 (mean = -0.0005 and s.d. = 0.003 for the GS study, mean = -0.0001 and s.d.
29 = 0.0007 for the NI study), variance of information (mean = -0.04 and s.d.
30 = 0.037 for the GS study, mean = -0.012 and s.d. = 0.004 for the NI study),
31 and distance correlation (mean = -0.037 and s.d. = 0.026 for the GS study,
32 mean = -0.0009 and s.d. = 0.0038 for the NI study). These statistics were
33 computed across the 110 original ROIs.

34 Below is a list of the equations for each measure considered.

35 For two classes represented as vectors

$$X = (x_1, x_2, \dots, x_n) \in \mathbb{R}^n$$

1 and

$$Y = (y_1, y_2, \dots, y_n) \in \mathbb{R}^n$$

2 where each component is computed as the arithmetic mean across m
 3 observations (trial-by-trial β coefficients) per class, per run, and n is the
 4 number of voxels. This notation is valid except for where these vectors show
 5 subscripts denoting individual observations as opposed to mean vectors (this
 6 is only the case when discussing distance correlation).

7 *Dot product*

$$XY^T$$

8 *Cosine distance*

9 The (negative) cosine distance is:

$$-(1 - \frac{XY^T}{\|X\|_2\|Y\|_2})$$

10 where $\|\cdot\|_2$ denotes the L2 (Euclidean) norm.

11 *Minkowski distance*

12 The (negative) Minkowski distance is:

$$-\left(\sum_{i=1}^n |x_i - y_i|^p\right)^{1/p}$$

13 For the city-block distance $p = 1$, for the Euclidean distance $p = 2$, and
 14 for the Chebyshev distance $p = \infty$.

15 *Pearson correlation*

$$\frac{\sum_{i=1}^n (x_i - \bar{x})(y_i - \bar{y})}{\sqrt{\sum_{i=1}^n (x_i - \bar{x})^2} \sqrt{\sum_{i=1}^n (y_i - \bar{y})^2}}$$

16 where \bar{x} and \bar{y} are the component-wise arithmetic means of vectors X
 17 and Y , respectively.

1 *Spearman correlation*

$$1 - \frac{6 \sum_{i=1}^n (rg(x_i) - rg(y_i))^2}{n(n^2 - 1)}$$

2 where $rg(x_i)$ and $rg(y_i)$ are the ranks of the values x_i and y_i , respectively.
3 This formulation assumes distinct integer rankings.

4 *Mahalanobis distance*

5 The (negative) Mahalanobis measure between two random vectors coming
6 from the same multivariate normal distribution is:

$$-\sqrt{(X - Y)^T \Sigma^{-1} (X - Y)}$$

7 where Σ is the $n \times n$ covariance matrix between voxels.

8 *Bhattacharyya distance*

9 The (negative) Bhattacharyya measure between two multivariate normal
10 distributions $\mathcal{N}(X, \Sigma_X)$ and $\mathcal{N}(Y, \Sigma_Y)$, where each voxel covariance matrix
11 Σ_X and Σ_Y is estimated separately for each class X and Y , respectively, is:

$$-\left(\frac{1}{8}(X - Y)^T \bar{\Sigma}^{-1} (X - Y) + \frac{1}{2} \ln \left(\frac{\det \bar{\Sigma}}{\sqrt{\det \Sigma_X \det \Sigma_Y}} \right)\right)$$

12 where

$$\bar{\Sigma} = \frac{\Sigma_X + \Sigma_Y}{2}$$

13 *Distance correlation*

14 The distance correlation is equal to 1 when X and Y span the same
15 linear subspace under some linear transformation and 0 when X and Y are
16 independent. It is defined as:

$$\frac{dCov(X, Y)}{dVar(X)dVar(Y)}$$

17 where $dCov^2(X, Y)$ is

$$\frac{1}{m^2} \sum_{j=1}^m \sum_{k=1}^m A_{j,k} B_{j,k}$$

1 and $dVar^2(X)$ is

$$\frac{1}{m^2} \sum_{j=1}^m \sum_{k=1}^m A_{j,k}^2$$

2 where $A_{j,k}$ is the matrix computed from doubly-centering the matrix $a_{j,k}$
3 (subtracting row and column means while adding the grand mean), where

$$a_{j,k} = \|X_j - X_k\|_2$$

4 Thus, $B_{j,k}$ is computed from $b_{j,k}$, where

$$b_{j,k} = \|Y_j - Y_k\|_2$$

5 These pairwise distance matrices are computed from distances between
6 observations.

7 *Variation of information*

8 For two classes X and Y represented as two multivariate Gaussian dis-
9 tributions, the (negative) Variation of information is

$$VI(X; Y) = I(X; Y) - H(X, Y)$$

10 where $H(X)$ is the entropy of X and $I(X; Y)$ is the mutual information
11 between X and Y .

12 For a multivariate Gaussian X , $H(X)$ is:

$$\frac{1}{2} \ln(\det(2\pi e \Sigma_X)) * n$$

13 where n is the number of observations. The mutual information between
14 X and Y is:

$$\frac{1}{2} \ln\left(\frac{\det \Sigma_X \det \Sigma_Y}{\det \Sigma^*}\right)$$

15 where Σ^*

$$= \begin{bmatrix} \Sigma_X & \Sigma_{XY} \\ \Sigma_{YX} & \Sigma_Y \end{bmatrix}$$

16 and Σ_{XY} is the between-class voxel covariance matrix. Σ_{YX} is the trans-
17 pose of Σ_{XY} .

1 *Covariance matrix regularization*

2 Two types of covariance matrix regularization were used for the Mahalanobis distance: diagonal regularization and Ledoit-Wolf regularization.

4 *Diagonal regularization*

5 Diagonal regularization for a covariance matrix Σ was computed as $\Sigma \circ I$,
6 where \circ is the hadamard product (element-wise multiplication) and I is the
7 identity matrix.

8 The distance measure that comes as a result of this type of regularization,
9 when applied to the covariance matrix of the Mahalanobis distance, is also
10 known as the normed Euclidean distance.

11 *Ledoit-Wolf regularization*

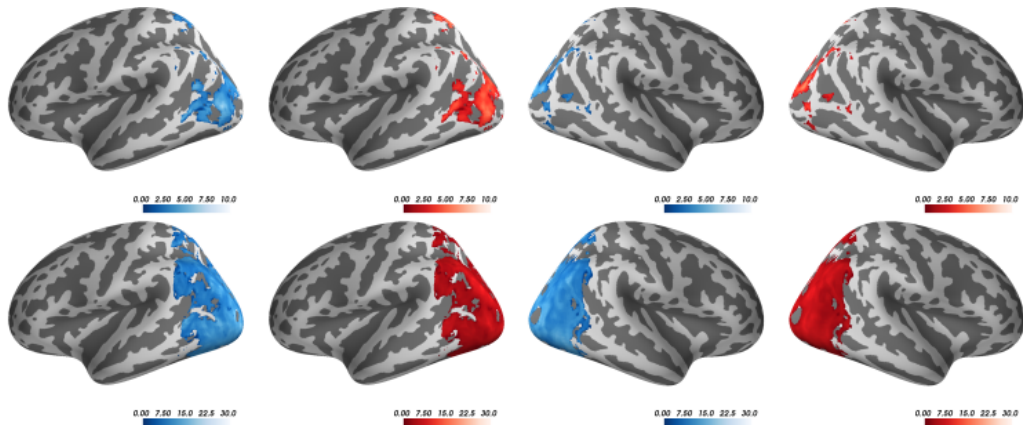
12 Ledoit-Wolf regularization for a covariance matrix Σ was computed as:

$$(1 - \text{shrinkage})\Sigma + (\text{shrinkage})(\mu)I$$

13 where $\mu = \text{trace}(\Sigma)/n$ and the optimal shrinkage parameter is a value
14 between 0 and 1 estimated according to the derivation in [5].

15 *E. Post hoc searchlight analysis*

16 Supplementary Figure 1 presents voxels where both the Euclidean measure
17 and the Mahalanobis(r) measure outperformed Pearson correlation.



Supplementary Figure 1: Voxels where Euclidean & Mahalanobis(r) overlap (outperforming Pearson). Lateral views of the left and right hemispheres for the GS study (top row) and the NI study (bottom row) displaying t statistics where both the Euclidean measure (blue) and the Mahalanobis(r) measure (red) outperformed the Pearson correlation measure. The t statistics were based on a searchlight analysis of Spearman correlations of each measure with each voxel's SVM confusion matrix (see Materials and Methods). Only displaying t statistics where $p < 0.001$ for paired sample t -tests, TFCE corrected; computed with FSL's randomise function with 5000 permutations, using as a mask the 12 ROIs with best accuracy (see Materials and Methods).

1 References

2 [1] M. Jenkinson, C. F. Beckmann, T. E. J. Behrens, M. W. Woolrich, S. M.
3 Smith, Fsl, *Neuroimage* 62 (2012) 782–790.

4 [2] J. A. Mumford, B. O. Turner, F. G. Ashby, R. A. Poldrack, Decon-
5 volving BOLD activation in event-related designs for multivoxel pattern
6 classification analyses, *Neuroimage* 59 (2012) 2636–2643.

7 [3] F. Pereira, T. Mitchell, M. Botvinick, Machine learning classifiers and
8 fMRI: A tutorial overview, *NeuroImage* 45 (2009) S199–S209.

9 [4] R. N. Shepard, Toward a universal law of generalization for psychological
10 science, *Science* 237 (1987) 1317–1323.

11 [5] O. Ledoit, M. Wolf, A well-conditioned estimator for large-dimensional
12 covariance matrices, *Journal of multivariate analysis* 88 (2004) 365–411.

13 [6] F. Pedregosa, G. Varoquaux, A. Gramfort, V. Michel, B. Thirion,
14 O. Grisel, M. Blondel, P. Prettenhofer, R. Weiss, V. Dubourg, Scikit-
15 learn: Machine learning in Python, *Journal of Machine Learning Re-
16 search* 12 (2011) 2825–2830.